Surface Stability in Liquid-Crystalline Block Copolymers with Semifluorinated Monodendron Side Groups

Maoliang Xiang,[†] Xuefa Li,[†] Christopher K. Ober,*[,†] Kookheon Char,[†] Jan Genzer,[‡] Easan Sivaniah,[‡] Edward J. Kramer,[‡,§] and Daniel A. Fischer[⊥,#]

Materials Science & Engineering, Bard Hall, Cornell University, Ithaca, New York 14853-1501; Department of Materials, University of California at Santa Barbara, Santa Barbara, California 93106; Department of Chemical Engineering, University of California at Santa Barbara, Santa Barbara, California 93106; Materials Science & Engineering Laboratory, National Institute for Standards and Technology, Gaithersburg, Maryland 20899; and NSLS, Brookhaven National Lab, Upton, New York 11973

Received December 16, 1999; Revised Manuscript Received April 24, 2000

ABSTRACT: Block copolymers with semifluorinated monodendron side groups were synthesized by attachment of a first generation 2- or 3-armed monodendron acid chloride to a hydroxylated poly(styrene-*b*-1,2/3,4-isoprene). A convergent growth strategy was developed to synthesize the monodendron groups in good yield using an approach that could be extended to higher generation monodendrons. High extents of attachment were achieved despite the steric effects of the bulky monodendron side groups. The resulting polymers formed a smectic B mesophase at room temperature as determined by WAXS data. The transition temperatures, mesophase range, and enthalpy of the smectic B−isotropic transition were all affected by side-group structural factors such as flexible spacer length, mesogen length, and monodendron core. The critical surface tensions of the resulting semifluorinated polymers were as low as ∼8 mN/m as determined by Zisman analysis. Surface stability of polymer films in a polar liquid environment was strongly dependent on the extent of attachment exhibited by the semifluorinated groups. The monodendron $-CF_2-$ helix within 1 nm of the surfaces has a net orientation normal to the surface as measured by near-edge X-ray absorption fine structure (NEXAFS) methods, but the orientational order parameter S_{helix} is much higher for the 2-armed monodendrons than for the 3-armed monodendrons. In both cases S_{helix} seems insensitive to monodendron attachment density along the isoprene block. We suggest that packing frustration of the monodendron subunits produces surfaces with spontaneous curvature that differs depending on whether the monodendrons are 2- or 3-armed. The more highly curved surface topology of the 3-armed monodendrons may provide a partial explanation for its decreased orientational order.

Introduction

This paper describes the synthesis and surface properties of a series of block copolymers containing pendent semifluorinated groups with a monodendron structure. The synthetic procedure involved monodendron group attachment to the isoprene block of a presynthesized block copolymer of styrene and isoprene. This strategy aided processing and organic solvent solubility of these new fluorinated polymers. The resulting materials were examined using a variety of methods including near edge X-ray absorption fine structure (NEXAFS) and contact angle studies and were shown to have stable, nonreconstructing surfaces in polar aqueous environments. These polymers possess stable nonreconstructing surfaces that depend on the mesomorphic character of these side groups and their extent of attachment.

Creating a compliant (elastomeric) polymer surface that does not reconstruct in changing environments is normally a difficult challenge. Such behavior is, however, of great interest in many applications of synthetic polymers ranging from simple protective coatings to release agents to biologically stable surfaces. In particular, the materials with the most interest, those with low-energy surfaces, often have the greatest thermodynamic driving force for reconstruction when in contact with a polar liquid as such as water. In the early 1960s, Zisman et al.[1] showed that the critical surface energy of fluoropolymers such as perfluorooctyl methacrylate polymers can reach as low as 11 mJ/m^2. Lindner[2] has, for example, recently synthesized a fluorinated silicone via the hydrosilylation reaction of fluorinated 1-olefins with poly(hydromethylsiloxane) and formed a material with a surface energy approaching 11 mJ/m^2 and at the same time demonstrated the feasibility of its nonwetting, low-energy surface to resist fouling by marine organisms. Thomas et al.[3] reported that water- and oil-repellent surfaces could be obtained even though the incorporation of fluorinated monomer in a methacrylate copolymer was as low as 1.5 wt %. To the best of our knowledge, there is little information on long-term surface stability reported in these studies.

Silicone- and fluorine-containing polymers are usually quite susceptible to rapid surface rearrangement. Since our goal is the creation of low surface energy materials for long-term use in a polar environment, a critical question is how the surface properties of polymeric materials can remain stable. Several approaches to creating stable surfaces have been successfully examined previously and include the creation of a network scaffolding immediately below the low-energy surface[4] and the stabilization of the surface using liquid crystalline groups.[5] Of special interest are polymers with semifluorinated (SF) side groups, that is, short segments of alkyl and perfluoroalkyl groups of 5−10 carbons each.[5,6]

[†] Cornell University.
[‡] Department of Materials, UCSB.
[§] Department of Chemical Engineering, UCSB.
[⊥] National Institute for Standards and Technology.
[#] Brookhaven National Lab.

10.1021/ma992111s CCC: $19.00
Published on Web 07/12/2000

The synthesis and structure of low molar mass semifluorinated materials were studied in detail by Rabolt et al.,[7] who first recognized the mesogenic character of short $-CF_2-$ segments. In subsequent study of several semifluorinated alkanes, Mahler[8] and Viney[9] generally found a common phase sequence on heating from a crystalline or highly ordered liquid crystalline phase to a smectic B phase. The properties of such semifluorinated materials can be used for tailoring surfaces by taking advantage of the stability of their ordered mesomorphic structure. In the case of semifluorinated LC groups, there is the advantage that not only does the surface resist reconstruction, but the mesomorphic structure presents a terminal $-CF_3$ group to the air and produces a very low energy surface (8−10 mJ/m^2).

Semifluorinated Groups: Effect of Mesophase on Surface Properties. There are only a few reports of semifluorinated polymers with LC character. Boileau et al.[6] reported the synthesis and low surface energy character of semifluorinated LC polysiloxanes made by hydrosilylation of poly(hydromethylsiloxane) with a semifluorinated LC vinyl compound. Semifluorinated methacrylate and acrylate polymers have been studied by Möller and co-workers[10] while their poly(vinyl ether) analogues have been synthesized by Percec.[11] All structures have in common low surface energies as demonstrated by advancing water contact angles in the range of 120°. Recently, we have successfully introduced semifluorinated groups onto one segment of a diblock copolymer backbone by using living anionic polymerization of poly(styrene-*b*-1,2/3,4-isoprene) followed by the appropriate polymer analogous reactions to the isoprene block.[5] It has been observed that such pendent semifluorinated segments retain the LC character of the small molecule when they are attached to a polymer backbone. It was found that the ratio of $-CF_2-$ and $-CH_2-$ groups significantly influenced both the LC and surface properties of the polymer. Segments of eight or more $-CF_2-$ carbons generally lead to formation of highly ordered, smectic B LC phases in which the $-CF_3$ surface groups are arranged in a hexagonal array. More importantly, this arrangement was found to be particularly stable against surface reconstruction in a polar environment. The uniform, semifluorinated LC surface composed of $-CF_3$ groups has high stability, because of the thermodynamic barrier to surface reconstruction provided by the LC phase.

Detailed analyses of semifluorinated surfaces using near edge X-ray absorption fine structure (NEXAFS) have shown that they are indeed dominated by $-CF_3$ end groups with the fluorinated segments projecting approximately normal to the surface.[12] In practice, however, semifluorinated units may not create a uniform $-CF_3$ layer on the surface if the substrate polymer is not completely substituted or the attachment sites are not densely spaced on the material surface. In this latter case, the perfluorinated chains may not be attached regularly enough to form the mesophase needed for a stable surface. Single semifluorinated side groups may also be unsuited for modification of preformed surfaces. Studies by our group of silicone surfaces modified with semifluorinated acid chlorides after network formation showed that they were susceptible to reconstruction, because of sparse substitution.[13] In other cases, the presence of underlying polar groups may lead to surface blooming and increase the polarity of surfaces.[14] We have therefore explored a monodendron strategy to address these issues of surface coverage and polar group masking by using the monodendron's larger surface coverage capability (see Scheme 1).

Scheme 1. Schematic of the Monodendron Semifluorinated Side Groups Studied as Well as the Single Semifluorinated Side Group for Comparison. Note the Relative Size of the Monodendron Side Groups as Well as Their Larger Coverage Area

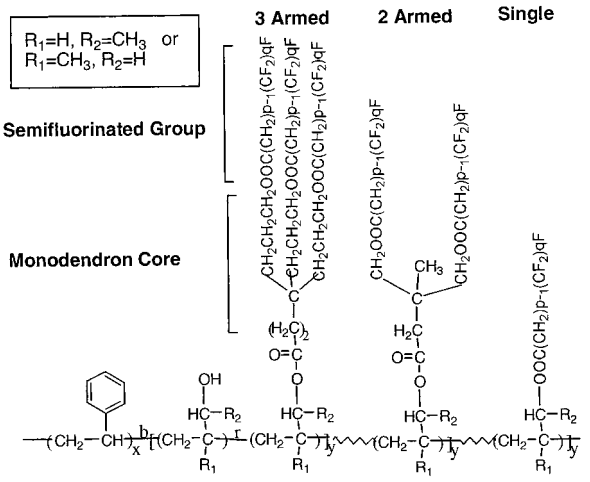

Dendrimers are a relatively new class of macromolecule. Recently monodendrons, a subunit of dendrimers, have been explored for surface modification. For example, monodendron monolayers have been successfully used as lithographic materials for patterning with SFM.[15] The advantage of such materials is that each monodendron can cover a large area per attachment site with each monodendron acting as an "umbrella" to cover and protect its portion of surface. Our goal as described in this report has been to examine semifluorinated monodendrons for surface coverage and the formation of stable, hydrophobic surfaces. Achieving this requires that the liquid crystalline SF groups form regular, organized structures on the surface.

This paper describes our recent efforts to prepare and characterize semifluorinated LC monodendron surfaces. In the design of the monodendrons, an all aliphatic, phenyl-free structure (see Schemes 2 and 3) was chosen in order to ensure that the substructure was sufficiently flexible and decoupled from a polymer backbone to permit ordering at the fluorinated surface. Both the surface properties and surface coverage effectiveness of the monodendron structure on one block of a block copolymer were examined. The surface structure, morphology, and thermal behavior of these polymers were studied by a combination of advanced analytical techniques including transmission electron microscopy (TEM) NEXAFS, differential scanning calorimetry (DSC), and SFM. The effect of the chemical structure of the monodendron core, the length of the fluorinated mesogen, and the flexible $-CH_2-$ spacer on the surface properties were of particular importance and are reported here.

Experimental Section

Materials. 5-Hexen-1-ol (99%), 9-decen-1-ol (98%), nitromethane trispropanol, 2,2-bis(hydroxymethyl)propionic acid, tributyltin hydride, and 10% Pd/C were used as received from Aldrich. Azobis(isobutyronitrile) (AIBN) was recrystallized from acetone/ethanol at 0 °C. Benzyl bromide and benzyl chloride from Aldrich were passed through a short column of activated aluminum oxide to remove any inhibitor prior to

Scheme 2. Synthesis of Semifluorinated 2-Armed Monodendron

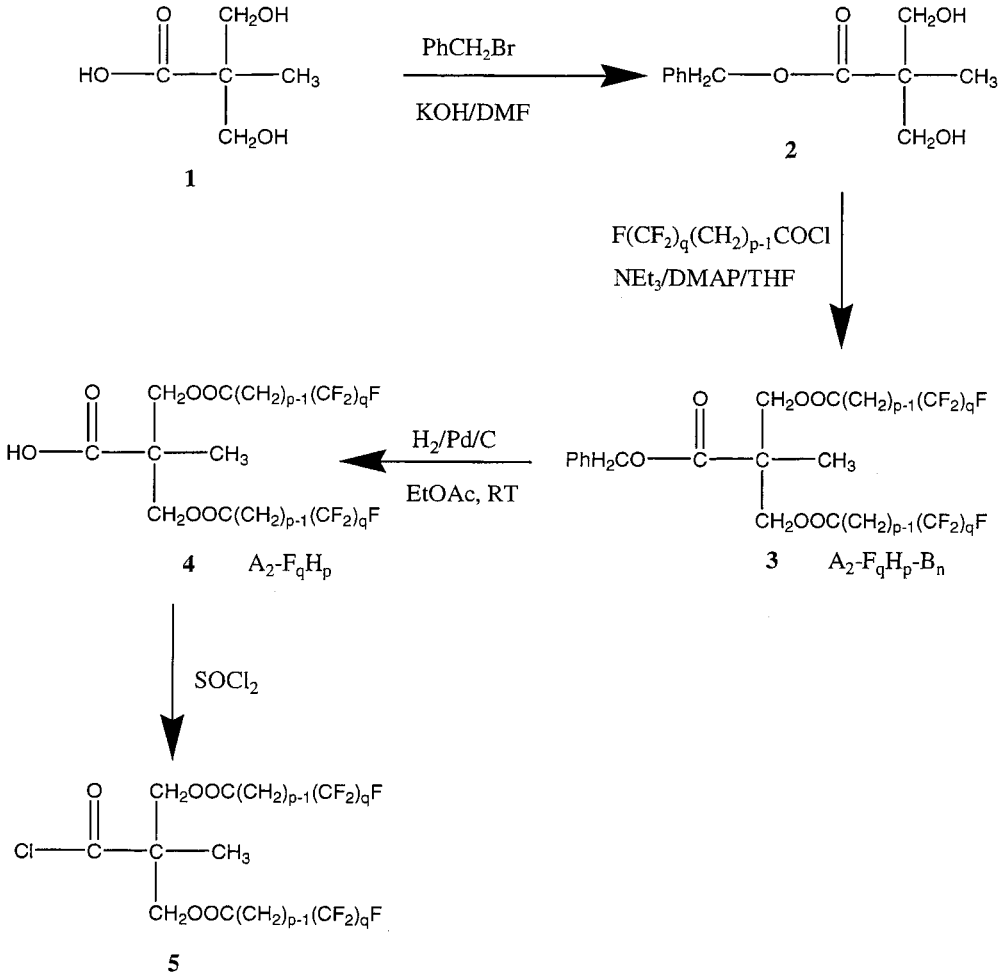

Scheme 3. Synthesis of Semifluorinated 3-Armed Monodendron

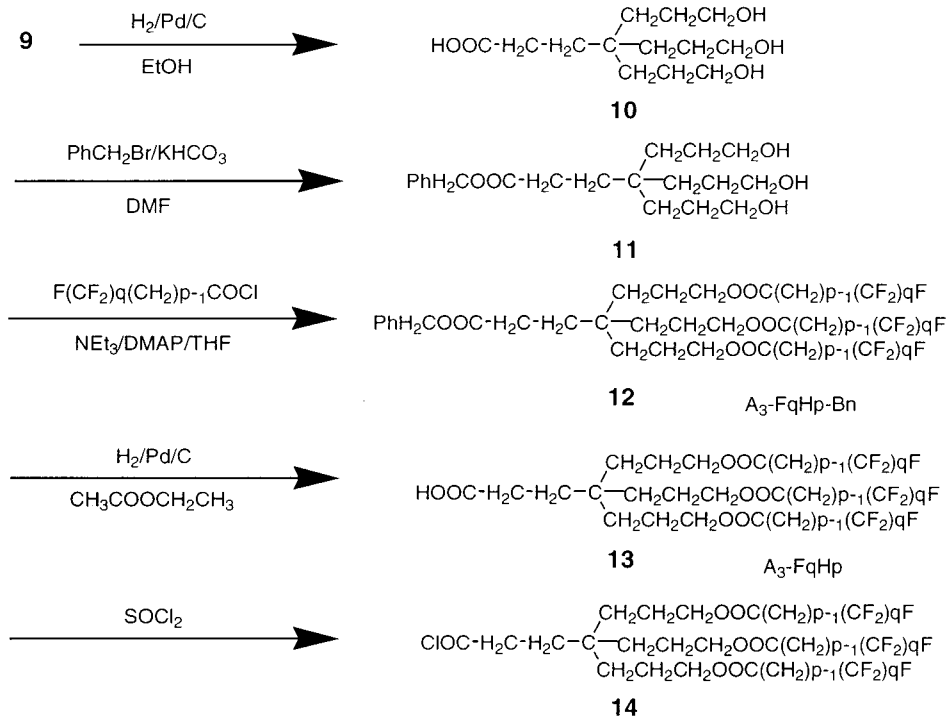

their use. Perfluorooctyl iodide (97%) and perfluorodecyl iodide (97%) were purchased from Lancaster Synthesis Inc. and used without further purification.

The procedures for synthesis of the block copolymers with semifluorinated monodendron side groups are shown in Schemes 2−4. Anionic polymerization was first carried out (see

Scheme 4. Attachment of Semifluorinated Monodendron Side Groups to Block Copolymers

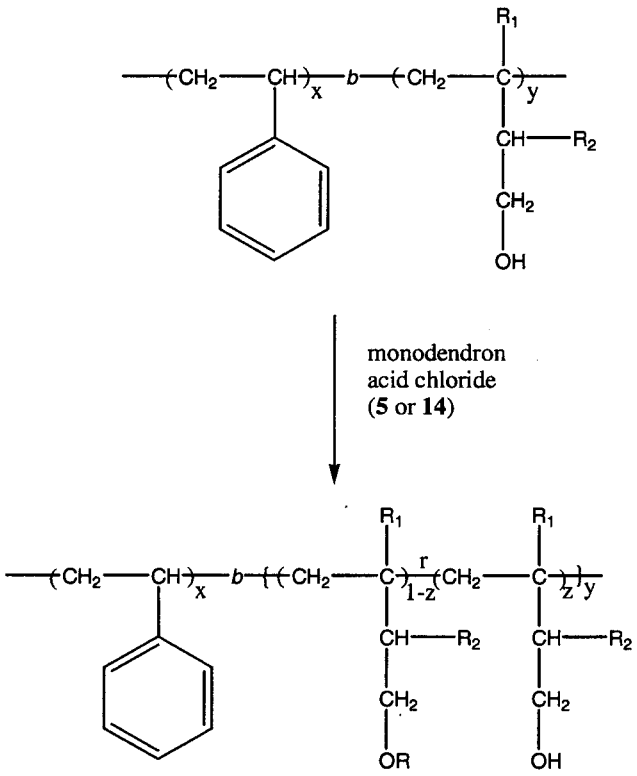

ref 5) followed by attachment of the monodendrons described below.

Synthesis of Benzyl Group Protected 2-Armed Monodendron. Benzyl-2,2-bis(hydroxymethyl)propionate (**2**) was synthesized by reaction of 2,2-bis(hydroxymethyl)propionic acid (**1**) with benzyl bromide in the presence of KOH in DMF in 65% yield, as described elsewhere.[13] The semifluorinated acid chlorides were synthesized from oxidation of semifluorinated alcohols, which can be readily prepared by the radical addition reaction of 1-iodoperfluoroalkane with ω-alken-1-ol, followed by treatment with thionyl chloride. Details of this synthesis can be found in a previous publication.[5]

To a 50 mL flask were added both 20 mL of anhydrous THF and 2.5 mL of anhydrous triethylamine (18.0 mmol) through a septum to dissolve 1.073 g of **2** (9.6 mmol OH) and 56 mg of (dimethylamino)pyridine (DMAP) which were previously placed in the flask. Upon cooling to 0 °C in an ice bath, 11.52 mmol of freshly distilled semifluorinated acid chloride (20% excess) was added dropwise using a syringe, leading to immediate formation of a white precipitate. Once addition was finished, the reaction was kept at this temperature for an additional hour, and then the reaction completed by stirring at 40 °C overnight. The reaction mixture was treated with 0.5 mL of water and extracted with dichloromethane. The organic phase was separated and neutralized with 0.1 N HCl solution until it reached pH 3. After washing the organic phase twice with water and then twice with 5% NaCl solution, the organic phase was dried over $MgSO_4$. Subsequently, the dichloromethane was evaporated, and the residual solid was purified by chromatography (ethyl acetate/hexane (v/v) 2/98−10/90). Compound **3** was then obtained as a white waxy solid in 90% yield.

Analysis of **2**. ^{1}H NMR ($CDCl_3$): δ 1.09 (s, 3H, $-CH_3$), 3.74 (d, 2H, $-CH_2OH$), 3.97(d, 2H, $-CH_2OH$), 5.20 (s, 2H, $-OCH_2$-Ph), 7.35 (bs, 5H, $-C_6H_5$).

Analysis of **3**. $A_2-F_8H_{10}-Bn$ ^{1}H NMR ($CDCl_3$): δ 1.0−1.75 (m, 31H, $-CH_3$ and $-CH_2-$), 2.04 (septet, 4H, $-CH_2CF_2-$), 2.24 (t, 4H, $-CH_2CO-$), 4.24 (d, 4H, $-CH_2OOCR$), 5.16 (s, 2H, $-OCH_2Ph$), 7.34 (bs, 5H, $-C_6H_5$).

Synthesis of 2-Armed Monodendron. To a 3 oz glass bomb with 1.5 g of **3** were added 15 mL of ethyl acetate and 0.15 g of 10% Pd/C catalyst. The system was purged with hydrogen several times using a water aspirator and maintained at 50 psi hydrogen at room temperature (RT) for 1 h. After filtration, the solution was concentrated and vacuum-dried to give **4** in 95% yield as a white powder.

Analysis of **4**. $A_2-F_8H_{10}$ ^{1}H NMR ($CDCl_3$): δ 1.0−1.75 (m, 31H, $-CH_3$ and $-CH_2$-), 2.04 (septet, 4H, $-CH_2CF_2-$), 2.24 (t, 4H, $-CH_2CO-$), 4.28 (d, 4H, $-CH_2OOCR$).

Synthesis of the Monodendron Acid Chloride (5). Compound **5** was prepared by reaction of the monodendron acid with thionyl chloride. As an example, 0.5 mL of thionyl chloride was added dropwise to a 10 mL round-bottomed flask charged with 1 g of monodendron **4**. After reacting at room temperature for 30 min, the reaction was heated to and maintained at 40 °C for 6 h. The excess $SOCl_2$ was removed by vacuum distillation at room temperature, followed by heating to 70 °C to give a yellowish solid, which was immediately used for attachment reaction without further purification.

General Procedure for Synthesis of 3-Arm Monodendron. The intermediates needed to make the 3-armed monodendron core (**6**−**9**) were synthesized as reported by Newkome et al.[17] The characterization data are identical to those previously reported.

Synthesis of 3-Armed Monodendron Core (10). Catalytic hydrogenation was used to obtain the monoacid triol (**10**). The same strategy was used for preparation of the 3-armed monodendron. To a 6 oz glass bomb containing 1.0 g of **9** were added 30 mL of absolute ethanol and 0.2 g of 10% Pd/C catalyst. The system was purged with hydrogen several times and vigorously stirred under 50 psi hydrogen at RT for 20 h. After filtration, the solvent was removed via vacuum distillation to give **10** in 90% yield as a white powder. In the ^{1}H NMR spectrum, proton resonances at 4.49 ppm (s, 6H, $-OCH_2$-Ph) and 7.29 ppm (m, 15H, $-C_6H_5$) disappear after this catalytic hydrogenation.

Analysis of **10.** ^{1}H NMR (DMSO-d_6): δ 1.0−1.75 (m, 14H, $-CH_2-$), 2.10−2.40 (m, 2H, $-CH_2COOH$), 3.42 (t, 6H, $-CH_2$-OH), 4.39 (t, 3H, $-CH_2OH$, disappeared upon addition of D_2O).

Synthesis of Benzyl Group Protected Triol (11). To a 100 mL round flask charged with 524 mg of **10** (2.0 mmol) and 220 mg of potassium bicarbonate (2.2 mmol, 10% in excess) was added 25 mL of anhydrous *N*,*N*-dimethylformamide (DMF). Upon addition of 0.285 mL of benzyl bromide (2.4 mmol, 20% in excess) in 1 mL of DMF through the septum, the reaction flask was wrapped with aluminum foil, and the reaction mixture was maintained at room temperature for 24 h. The potassium bicarbonate particles gradually become smaller over the course of the reaction. After the solvent was distilled under reduced pressure at 60 °C, the residue was subjected to column chromatography (from EtOAc to 10/90 methanol/EtOAc) to give **11** in 60% yield as colorless liquid.

Analysis of **11.** ^{1}H NMR (DMSO-d_6): δ 1.0−1.75 (m, 14H, $-CH_2-$), 2.10−2.40 (m, 2H, $-CH_2COOH$), 3.32 (t, 6H, $-CH_2$-OH), 5.07 (s, 2H, $-OCH_2C_6H_5$), 7.36 (bs, 5H, $-C_6H_5$).

Synthesis of 3-Armed Monodendron Acid Chloride (14). The benzyl protected monodendron (**12**) was synthesized in the same manner used to produce compound **3**. For synthesis of compound **13**, the same procedure for hydrogenation of **3** was also applied. However, in the case of compounds with $-CF_2-$ segments, 10 C long, a 1:1 mixture of dichloromethane and ethyl acetate was used instead of ethyl acetate

alone as solvent in order to enhance the solubility of the resultant monodendron acid. The corresponding monodendron acid chloride **14** was made in a manner similar to the 2-armed synthesis. All acid chlorides were used immediately for the attachment reaction.

Analysis of **12.** $A_3-F_8H_{10}-Bn$ ^1H NMR ($CDCl_3$): δ 1.0−1.75 (m, 56H, $-CH_2-$), 2.05 (septet, 6H, $-CF_2CH_2$), 2.29 (t, 8H, $-CH_2COO-$), 4.02 (t, 6H, $-CH_2OOC-$), 5.12 (s, 2H, $-OCH_2C_6H_5$), 7.36 (bs, 5H, $-C_6H_5$).

Analysis of **13.** $A_3-F_8H_{10}$ ^1H NMR ($CDCl_3$): δ 1.0−1.75 (m, 56H, $-CH_2-$), 2.05 (septet, 6H, $-CF_2CH_2$), 2.29 (t, 8H, $-CH_2$-COO−), 4.03 (t, 6H, $-CH_2OOC-$).

Synthesis of Block Copolymers with Semifluorinated Monodendron Side Groups. The hydroxylated poly(styrene-*b*-1,2/3,4-isoprene) was synthesized via sequential anionic polymerization of the corresponding monomers of styrene and isoprene and followed by hydroboration and oxidation under mild conditions. These details have been reported elsewhere.[5,18] Synthesis of single chain semifluorinated alcohols, acids, and acid chlorides was also reported in a previous publication.[5]

To a 10 mL flask with 0.2 g of hydroxylated polymer and 5 mg of DMAP dissolved in 0.5 mL of pyridine and 2 mL of CH_2Cl_2, the desired amount of freshly prepared 50 wt % monodendron acid chloride (**5** or **14**) in CH_2Cl_2 was then injected slowly through a rubber septum. Immediate precipitation could be observed. After the reaction was stirred at RT overnight, 1 mL of α,α,α-trifluorotoluene (TFT) was added if the solution was viscous and stirring was difficult. The polymer solution was poured into a 9:1 methanol/water solution after the reaction was heated to 40 °C and held at this temperature for 24 h more. The polymer powder was filtered and then dissolved in an appropriate solvent, such as THF, CH_2Cl_2, TFT, or a mixture of these solvents depending on the extent of attachment and LC mesogen. This dissolution−precipitation cycle was repeated four more times. After further extraction with hexane for 24 h using a Soxhlet extractor, the polymer was dried overnight at 60 °C in a vacuum oven.

Characterization of Polymers. Gel permeation chromatography (GPC) with four Waters Styragel HT columns was run at 30 °C, with monodisperse polystyrene as standard. The extent of attachment of the fluorinated side groups was calculated from ^1H NMR measurements that were carried out on a Varian 200 spectrometer. The thermal transitions were studied by differential scanning calorimetry (DSC) measurement using a Perkin-Elmer DSC-7 series instrument with a 10 °C/min heating and cooling rate.

Contact angles were determined with a NRL contact angle goniometer model 100-00 (Ramé-Hart Inc.) at room temperature. The samples were prepared by spinning 5 wt % copolymer/TFT solutions at a speed of 2500 rpm on a silicon wafer at room temperature or elevated temperature. Critical surface tension was measured using linear alkanes and low molecular weight trimethylsilyl-terminated poly(dimethylsiloxane)s (Gelest Inc.) as standards.[19]

Bulk samples of these block copolymers were prepared for TEM and small-angle X-ray scattering (SAXS) studies of microdomain structures. Films of thickness ∼1 mm were cast from 5 wt % solutions in TFT. The solvent was allowed to evaporate slowly for 1 week at room temperature. Then the as-cast film was dried thoroughly under vacuum at room temperature for 2 days to remove residual solvent and annealed at 145 °C under vacuum for 4 days to improve long-range order of the morphology. An annealing temperature of 145 °C was high enough (∼40 °C) above the glass transition of the PS block to allow mobility of the chains.

The annealed as-cast film was used for X-ray studies without further processing. X-ray experiments were performed at the Cornell High Energy Synchrotron Source (CHESS). The X-ray wavelength and intensity and the distance between the sample and CCD detector were easily adjusted according to experimental need.

For TEM studies, small pieces of as-cast films were embedded in epoxy resin which was cured at 70 °C for 6 h to produce samples suitable for cross-sectional microtoming. Thin sections were microtomed at room temperature and stained with RuO_4 for 15−20 min (RuO_4 preferentially stains PS microdomains). A JEOL 1200EX transmission electron microscope operated at 120 kV was used in this study.

Infrared spectra were measured with a Mattson 2020 Galaxy Series FTIR with 4 cm^{-1} resolution averaging 64 scans. Samples were either cast onto a NaCl crystal plate, pressed in a KBr pellet, or made in a thin liquid film between two NaCl crystal plates.

The NEXAFS experiments were carried out on the NIST/Dow materials characterization end station on the U7A beamline at the National Synchrotron Light Source at Brookhaven National Laboratory. A toroidal mirror spherical grating monochromator gives this beamline an incident photon energy resolution and intensity of 0.2 eV and 5×10^{10} photons/s, respectively, for an incident photon energy of 300 eV and a typical storage ring current of 500 mA. The X-rays are elliptically polarized, with the electric field vector **E** dominantly in the plane of the storage ring (polarization factor = 0.85). The monochromator energy and resolution were calibrated by comparing the transmission spectrum from gas-phase carbon monoxide with electron energy loss reference data.

For the NEXAFS experiments polymer films approximately 200 nm thick were prepared by spin-casting onto silicon wafers from trifluorotoluene solutions and annealed for 6 h in a vacuum at 150 °C. A goniometer stage allowed the angle of the sample surface with regard to the polarization vector of the soft X-rays to be varied between 20° and 90°. Our NEXAFS experiments measure the resonant soft X-ray excitation of a carbon 1s electron to a σ^* orbital, an unoccupied low-lying antibonding molecular orbital with σ symmetry.[14] Since the $1s \rightarrow \sigma^*$ resonant excitations are governed by dipole selection rules, the transitions are polarized; i.e., their intensity varies as a function of the direction of the electric field vector **E** of the incident X-ray photon relative of the long axis of the σ^* orbital of the final state. In our experiments we detect the resonant excitation by monitoring the emission of Auger electrons from the near surface region of the polymer film. These Auger electrons form most of the partial electron yield (PEY) signal that is collected using a channeltron electron multiplier that has an adjustable entrance grid bias (EGB). Auger electrons that have lost significant energy in emerging from more than 2 nm below the surface are discriminated against by increasing the negative EGB on the channeltron detector. To eliminate the effect of incident beam intensity fluctuations and monochromator absorption features, the PEY signal was normalized by the incident beam intensity obtained from the photoyield of a clean gold grid.

Results and Discussion

Direct syntheses of fluorinated block copolymers have been reported by a number of living polymerization methods.[10,11] However, direct anionic polymerization of fluorinated monomers cannot be readily undertaken due to their poor solubility in common solvents at low temperature as well as the sensitive character of chemical functions associated with many fluorinated groups. In this study, the semifluorinated monodendron groups were therefore attached to preformed polymers using the esterification chemistry that has been successfully demonstrated with styrene-modified diene block copolymers.[5] A great advantage of this postpolymerization chemistry is that a single base polymer with a well-defined block copolymer architecture can be reliably prepared in a large quantity via living anionic polymerization and then modified with different side groups. This approach enables the direct comparison of different side groups on the same polymer backbone.

Synthesis of Semifluorinated Monodendrons. In this paper, a protection−deprotection procedure and convergent growth strategy were used for synthesis of the target monodendrons. The large differences in

molecular weight and polarity between products and starting materials or byproducts made purification much simpler. In the synthetic schemes employed, two major reaction steps, esterification of protected intermediates and deprotection via hydrogenation, were used. Ester formation was carried out in very high yield through acid chloride chemistry in the presence of base (triethylamine or pyridine) and (dimethylamino)pyridine (DMAP) catalyst. A benzyl function was used as a protecting group because it can be cleanly and quantitatively removed by catalytic hydrogenation.[20] In addition, this hydrogenation step does not cleave the ester bonds formed between the monodendron core and the single semifluorinated segments.[16] On the basis of these reaction steps, we have successfully synthesized 2-armed and 3-armed single generation semifluorinated monodendrons in good yields.

Prior to producing the 2-armed monodendron, we recognized that **4** can also be obtained from the direct one-step reaction of **1** and a semifluorinated acid chloride. However, there are possible acid chloride exchange reactions, and as a consequence, an intermolecular esterification reaction may occur between two molecules of **1**. In addition, the final monodendron acid is extremely difficult to separate from any free semifluorinated acid produced from the excess semifluorinated acid chloride, because the physical properties of these two acids are very similar. Despite the three reaction steps involved in Scheme 1, the benzyl-protected monodendron is easily purified from the single semifluorinated acid by chromatography in step two. Because of the inexpensive starting material **1** and the efficient esterification and debenzylation reactions, this multistep scheme is considered to be much better than the direct reaction in making the pure monodendron.

For the synthesis of the 3-armed monodendron core, the first three steps were adapted from ref 17. Quantitative hydrogenation of the benzyl ester at relatively low pressure was used in the final step. Absolute ethanol was chosen as the solvent since the resulting product **10** was expected to be very hydrophilic. Because of the relatively high reactivities of both hydroxyl and carboxyl groups in **10** and the low vapor pressure of ethanol, it was necessary to avoid high reaction temperatures during the removal of the solvent in order to prevent any possible side reactions such as unwanted esterification. However, this reaction has the additional advantage of easy workup and pure product formation because the activated carbon present as the catalyst support can absorb impurities in the starting material.

For the reasons mentioned above, the monodendron core **10** was converted to its benzyl ester **11** within 24 h of synthesis to avoid any side reactions during storage. Initially, we used the same reaction conditions (KOH/DMF, 100 °C) as for the 2-armed monodendron reaction. However, the resultant product was a viscous liquid. ^{1}H NMR analysis showed the existence of both benzyl and other aliphatic esters. A possible cause was the vigorous reaction conditions used. An efficient method of esterification has been reported by Pfeffer et al.[21] through alkylation of carboxylate salts with alkyl halides in dipolar aprotic solvents. To avoid side reactions, very mild reaction conditions ($KHCO_3$, $C_6H_5CH_2Br$, RT) were chosen. The corresponding potassium monodendron carboxylate, which is formed in situ using potassium bicarbonate, reacts immediately with the more reactive benzyl bromide (instead of benzyl chloride) to give the corresponding benzyl group protected triol. Dark reaction conditions were used to reduce the possibility of photolysis of benzyl bromide and to make final separation easier. Irreversible evolution of carbon dioxide favors product formation. Thin-layer chromatography (TLC) was used to monitor the conversion of the acid to benzyl ester. Through combination of both reduced base strength and reaction temperature, no evidence of ester formation between the hydroxyl and carboxyl groups was detected in ^{1}H NMR measurement. The polarity difference between **10** and **11** makes separation simple by chromatography. For the case of the 3-armed monodendron **13** with a $-CF_2-$ length of 10, the resultant monodendron was insoluble in ethyl acetate. It was necessary to reduce the polarity of the solvent by using a mixed solvent of dichloromethane and ethyl acetate.

Synthesis of Semifluorinated Block Copolymers. Several factors, such as monodendron attachment chemistry, the type of monodendron, and the solvent system, were examined for their influence on the attachment efficiency of the semifluorinated monodendron. The use of acid chloride (**5** or **14**) for attachment to the hydroxylated block copolymer backbone was found to be the most efficient reaction. Complete removal of excess thionyl chloride from the monodendron acid chloride was critical in order to avoid chlorination of any hydroxyl group on the polymer backbone during the attachment reaction. Because of the large molecular weight of the monodendron acid chloride, we elected to heat the resultant acid chloride above its melting point under vacuum to remove residual thionyl chloride rather than risk partial hydrolysis during recrystallization.

The type of monodendron affects attachment efficiency. Under the best conditions, an attachment ratio (defined as the percentage conversion from hydroxyl group to monodendron ester) as high as ~80% could be reached for the 2-armed monodendron and up to ~60% for the 3-armed monodendron, even though an excess of monodendron acid chloride was used. Because of the bulkiness and solubility of the monodendron group, we believe steric hindrance played a significant role in attaining high conversion and restricted further attachment. The reaction medium had an important effect on the attachment ratio as well. Attachment in dichloromethane or THF lead to low conversion, simply because of the low solubility of the resultant polymer in such solvents. Immediate addition of a nonpolar solvent, such as trifluorotoluene (TFT), leads to precipitation of the starting hydroxylated polymer, which is quite polar. As a result, a two-stage procedure was developed to achieve higher attachment levels. In the first stage, excess pyridine was used as a hydrochloric acid acceptor and a solvent for the hydroxylated polymer. Because of the low solubility of the monodendron acid chloride, the reaction system gradually gelled, indicating the occurrence of the attachment reaction. In the second stage after the initial 12 h reaction period, some of hydroxyl groups have been converted to the less polar monodendron ester. It was usually necessary at that point to increase the reaction temperature and add nonpolar solvent, such as TFT, to enhance the solubility of the resulting polymer and achieve higher attachment levels.

Attachment of monodendron side groups could be confirmed by the downfield shift of the CH_2O- group on the isoprene block by ~0.4 ppm, which indicates the formation of monodendron ester from the corresponding

Table 1. Molecular Weight and Composition Analysis of Semifluorinated Block Copolymers with F_8H_{10} Single and Monodendron Side Groups

polymer[a]	side group	starting PS/PI	attachment ratio	calcd MW of final polymer	obsd from GPC	peaks
BC-0.99F8H10	F_{8H10}	41.1K/7.3K	full	41.1K/70.6K	81.0K	two
BC-0.52F8H10	F_{8H10}	41.1K/7.3K	51.9%	41.1K/41.2K		one
BC-3A0.59F8H10	A_3-F_8H_{10}	38.2K/6.7K	58.5%	38.2K/121.4K	3000K	two
BC-3A0.56F8H10	A_3-F_8H_{10}	66K/5.5K	56.2%	66K/96K		

[a] BC denotes block copolymer, FxHy refers to the composition of the semifluorinated group, and 0.*zz* indicates the extent of attachment on the hydroxylated backbone.

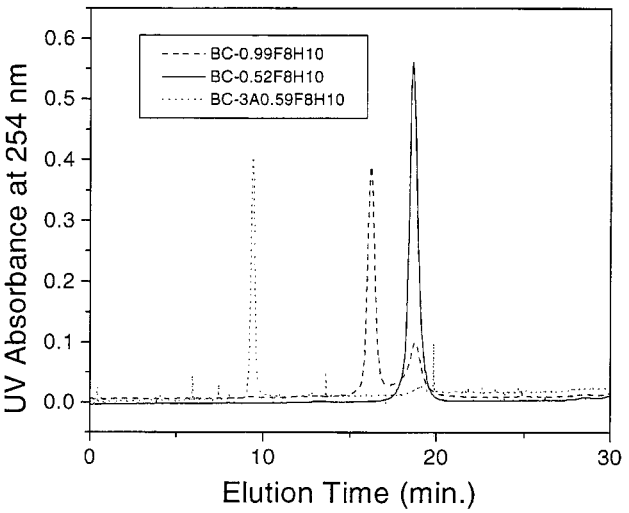

Figure 1. GPC traces of semifluorinated block copolymers with 3-armed monodendron and single SF side groups with different extents of attachment (measurements made in THF) showing both free chains and micellar structures: BC-0.99F8H10 (- - -), BC-0.52F8H10 (—), and BC-3A0.59F8H10 (• • •).

alcohol. The FTIR spectra showed very strong $-CF_2-$ stretching bands between 1150 and 1250 cm^{-1} and a very weak OH stretching band around 3400 cm^{-1}, indicating the existence of C−F bonds and residual OH groups. An attachment ratio, determined by ^1H NMR measurement in $CDCl_3$, was always found to be smaller than expected. Since the modified polyisoprene block is not readily soluble in such solvents, the semifluorinated polymer tends to form micellar structures in solution (see discussion below). Thus, a nonpolar solvent trifluorotrichloroethane was added as a cosolvent to enhance the solubility of semifluorinated block copolymer to obtain the correct attachment ratio.

Solution Properties of the Semifluorinated Polymers. The solubility of these semifluorinated block copolymers with monodendron side groups depends strongly on a combination of the $-CF_2-$ length, extent of attachment, and the composition of the block copolymer. With attachment levels greater than 50%, the semifluorinated polymer was soluble only in nonpolar solvents such as TFT and slightly soluble in solvents such as THF, toluene, and chloroform. If the $-CF_2-$ length was 10, the semifluorinated polymer was only soluble in hot trifluorotoluene. As mentioned above, ^1H NMR measurement of the semifluorinated polymer in chloroform gives an incorrect extent of attachment even though the polymer appears soluble and forms a transparent solution.

As shown in Figure 1, generally two peaks are observed by GPC for the semifluorinated monodendron polymer when the $-CF_2-$ mesogen length is longer than 8 and the extent of attachment is higher than 25%. This is similar to observations made in previous studies[5] of a polymer (BC-0.99F8H10) with single semifluorinated side groups. It is known that micellization of block copolymers generally occurs in a solvent that is selective for one block but is a poor solvent for the other block.[22] The higher molecular weight peak observed in Figure 1 is associated with micelle formation while the lower molecular weight peak is due to the isolated block copolymer molecules. For comparison, we synthesized polymer with single semifluorinated side groups (BC-0.52F8H10) with a similar attachment ratio (but clearly lower F content) to a polymer with 3-armed monodendrons (BC-3A0.59F8H10), so that it had the same molar ratio of residual OH groups, as listed in Table 1. BC-0.52F8H10 does not form micelles under these conditions as judged from the GPC trace (Figure 1), while the polymer with semifluorinated monodendron side groups (BC-3A0.59F8H10) shows very strong micellization behavior with only a small fraction of free polymer chains. The ratio of micellar to free chains of this polymer is higher than BC-0.99F8H10 (full attachment), as can be seen from Figure 1. The overall content of $-CF_2-$ groups in a polymer plays a very important role in this micellization behavior since the residual OH group content remains the same. Prior published work [5] has shown that no micellization occurs if the $-CF_2-$ length is 6 or less, independent of the extent of attachment. Details of the micellar structure are being investigated by light scattering and other methods. Even though the presence of micelles can be readily demonstrated in many of these polymers, the surface properties did not depend on the casting solvent.

LC Behavior in a Monodendron Structure

Dendrimers and monodendrons have recently received intense study either as single molecular species[23,24] or attached to polymer chains[25−27] to form so-called bottle brush polymers. Focusing on fluorinated dendrimer structures, DeSimone and co-workers[28] have reported fourth generation poly(ethylenimine)s with a "CO_2-philic" shell derived from a heptamer acid fluoride of hexafluoropropylene oxide that act as excellent surfactants in CO_2 media. Percec and co-workers[29] have reported the self-assembly behavior of a homopolymer with semifluorinated monodendron side groups. However, its LC mesophase was quite weak as judged by its low Φ_h−isotropic transition enthalpy (0.2−0.3 kcal/mol repeat unit). The same research group also[30] synthesized a series of semifluorinated tapered monodendrons, which were capable of forming supramolecular columnar structures with a homeotropic hexagonal columnar LC phase, and studied the fluorophobic effect on the self-assembly behavior compared with their hydrocarbon analogues. Since the fluorinated segments were connected to an aromatic core group, the ability of the SF structure to spontaneously organize into an ordered surface was unclear.

However, in other work by Percec,[31] dendrimers with conventional mesogenic groups and linking spacers were

Table 2. Thermal Analysis of Semifluorinated Block Copolymers with Monodendron Side Groups with Selected Semifluorinated Group Composition and Extents of Attachment

polymer[a]	monodendron	attachment ratio (%)	T (°C)	ΔH (J/g)
BC-2A0.62F8H6	A_2-F_8H_6	68.2	30.9	2.0
BC-2A0.66F8H10	A_2-F_8H_{10}	66.3	47.8	7.0
BC-2A0.38F10H10	A_2-$F_{10}H_{10}$	38.0	67.7	3.5
BC-3A0.24F8H10	A_3-F_8H_{10}	23.7	55.6	3.9
BC-3A0.53F8H10	A_3-F_8H_{10}	53.1	62.4	10.1
BC3A0.58F10H10	A_3-$F_{10}H_{10}$	57.5	95.4	11.6

[a] BC denotes block copolymer, FxHy refers to the composition of the semifluorinated group, and 0.*zz* indicates the extent of attachment on the hydroxylated backbone. Molecular weight of the starting PS/PI block copolymers is 38.2K/6.7K.

shown to form stable mesophases, thereby indicating that a mesogenic group can pack into an ordered structure when the appropriate dendrimer architecture is used. Lattermann and co-workers[32] reported the synthesis of dendrimeric poly(ethylenimine)s with 3,4-bis(decyloxy)benzoyl "2-armed" groups. Having a LC shell around a central nucleus, these dendrimers exhibited a variety of LC phases and a monotropic hexagonal columnar (Col_h) or enantiotropic Col_h phase if the imines are protonated. Thus, the prospects for creating low generation number LC monodendrons with strong surface order are excellent.

The LC behavior of the monodendron substituted polymers studied here was investigated using thermal analysis.All samples were first heated to 180 °C at 10 °C/min, held there for 5 min, and cooled to −60 °C at 10 °C/min rate to ensure formation of the mesophase. After samples were held at this temperature for another 5 min, DSC data were collected. In addition to the glass transition of the PS block at ∼102 °C, only a single first-order transition was found. This transition was reversible as indicated by a DSC cooling run, and on the basis of X-ray analysis, it can be assigned to a transition from the smectic B mesophase to the isotropic state. This is different from the behavior of single SF side groups attached to the same block copolymer in which two transitions were observed. One possible explanation for this difference is that introduction of a monodendron structure disturbs the formation of a mesophase. However, both the enthalpy of transition and the transition temperature are sensitive to not only the structure of the semifluorinated unit but also the monodendron core and the attachment ratio. Thermal data for the semifluorinated polymers are given in Table 2.

In the 2-armed monodendron series, when the CH_2 spacer length increases from 6 (BC-2A0.62F8H6) to 10 (BC-2A0.66F8H10), the transition temperature increased from ∼31 to 47.8 °C, and the transition enthalpy grew dramatically from 2.0 to 7.0 J/g. A similar enthalpy increase was found in the single SF side group case growing from 5.2 J/g (CH_2 6) to 10.3 J/g (CH_2 10).[5] This observation shows that increasing CH_2 spacer length improves self-assembly of the perfluorinated mesogenic unit. The advantage of monodendrons with an aliphatic core can be observed in a comparison to SF monodendrons with aromatic cores reported in the literature.[29] The transition enthalpy and thus the stability of the mesophase of monodendrons with an aromatic core is much lower (∼0.5 J/g, 8 $-CF_2-$, **21**-4/8) due to both a shorter spacer and the rigid aromatic core.

The transition temperature also depends on the length of the mesogenic $-CF_2-$ segment. When the $-CF_2-$.length increases from 8 to 10, this transition temperature increases significantly from 47.8 °C (BC-2A0.66F8H10, $F(CF_2)_8$) to 67.7 °C (BC-2A0.38F10H10, $F(CF_2)_{10}$) even though the latter polymer has a relatively low attachment ratio. In comparison with our previous work on single chain SF groups,[5] the 2-armed monodendron structure even with higher fluorine content in the polymer has a lower transition enthalpy than that of a fully attached polymer with the same semifluorinated unit. This demonstrates that a 2-armed monodendron core has a substantial effect on self-assembly of the semifluorinated unit, even though the transition temperature is comparable.

As can be seen from Table 2, the transition temperature for the 3-armed monodendron polymer is almost 25 °C higher than that for the corresponding 2-armed one, and the transition enthalpy for the 3-armed series is also much higher, if the attachment ratio is kept in the same range. From a structural viewpoint, the difference between the 3-armed and 2-armed monodendron cores is caused by the additional CH_2 groups present in the 3-armed case which provide extra conformational flexibility for the fluorinated segments to order into a well-ordered mesophase.

In addition, the attachment ratio was found to affect the transition enthalpy (3.9 J/g for BC-3A0.24F8H10 (24% attachment) versus 10.1 J/g for BC-3A0.53F8H10 (53% attachment)) but have little effect on transition temperature (55.6 °C for BC-3A0.24F8H10 versus 62.4 °C for BC-3A0.53F8H10). The monodendron side groups can form a similar, stable mesophase even at relatively low attachment levels; however, a lower transition enthalpy is an indication of decreased stability of the mesophase in the bulk. From the discussion above, it is believed that the CH_2 spacer plays an important role in determining the transition enthalpy while the $-CF_2-$ mesogen influences mostly the transition entropy (and thus the transition temperature without changing the transition enthalpy). In the next section, we discuss how this LC behavior affects the surface properties of a polymer film.

Solid State Properties of the Semifluorinated Polymers. The morphology of these polymers was examined by X-ray diffraction and transmission electron microscopy (TEM). BC-2A0.66F8H10, a 2-armed monodendron block copolymer, was selected as a representative polymer for thorough study. As shown in Figure 2, a highly ordered smectic mesophase is observed by WAXD analysis. Three orders of reflection can be clearly seen at spacings of 40, 20, and 13 Å and were assigned to the smectic layers. The two sharp, oriented outer arcs with a d spacing of 4 Å can be identified as the intermesogen spacing. The sharpness of the two outer arcs shows that d spacing between mesogens is very uniform and that they are oriented normal to the layers of the smectic mesophase. This feature is characteristic of a smectic B mesophase for this block copolymer. The theoretical length of this mesogen is about 21 Å estimated by computer simulation. Thus, within each layer of the mesophase, a model with two mesogens arranged head-to-head to make up the 40 Å layer thickness is consistent with observation.

TEM images of this sample (Figure 3) revealed a microphase-separated, highly organized and hexagonally packed cylinder morphology with PS cylinders placed in a fluorinated LC matrix, as expected from the

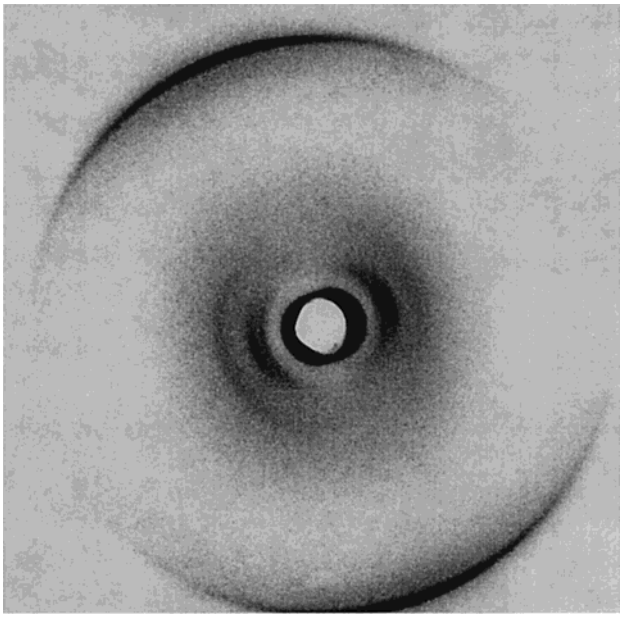

Figure 2. WAXD pattern of BC-2A0.66F8H10 2-armed monodendron diblock copolymer (66.2% attachment; λ = 1.03 Å, sample-to-detector distance = 111 mm).

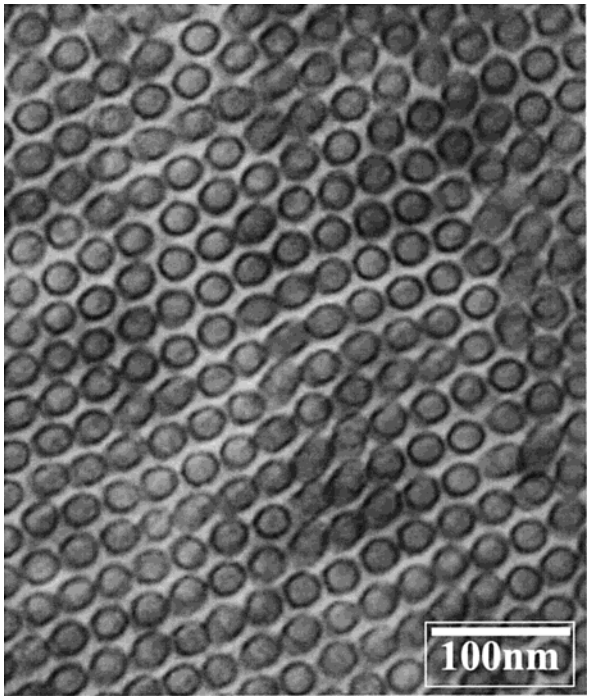

Figure 3. TEM micrograph of BC-2A0.66F8H10 2-armed monodendron diblock copolymer (66.2% attachment).

estimated volume fractions of the LC block (f_{LC} = 59.2%). The domain spacing (distance between cylinders) obtained from TEM was 670 Å, with a cylinder radius R of ~260 Å. The dark edge of the cylinder is believed to arise from preferential staining along the microstructure interface due to fast diffusion through the LC domain and slow diffusion into the PS one. To confirm this morphology, a two-dimensional SAXS pattern (Figure 4) was recorded. This highly oriented X-ray pattern also showed that macroscopically aligned films could be prepared by a simple solvent-casting process. A one-dimensional line scan of this pattern (Figure 5) clearly showed peaks of 100, 110 (as a shoulder), 200, and 210 indices in a ratio of 1:$\sqrt{3}$:$\sqrt{4}$:$\sqrt{7}$, which is

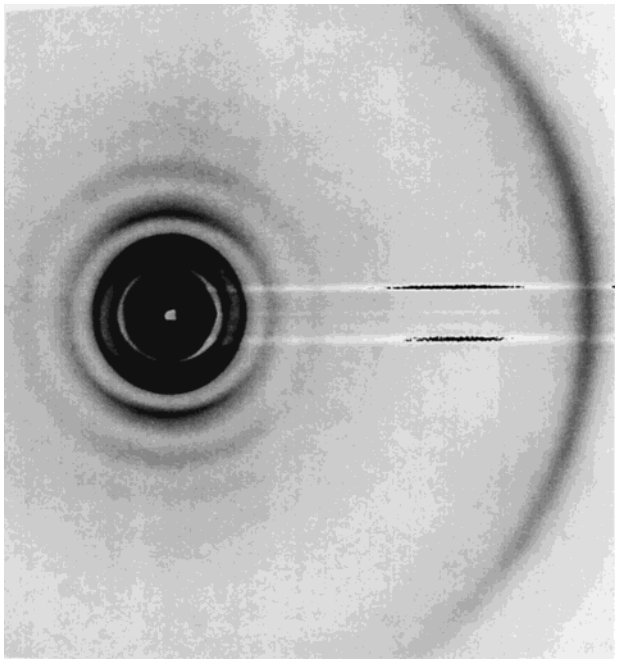

Figure 4. Two-dimensional SAXS pattern of BC-2A0.66F8H10 (λ = 1.54 Å; sample-to-detector distance = 828 mm).

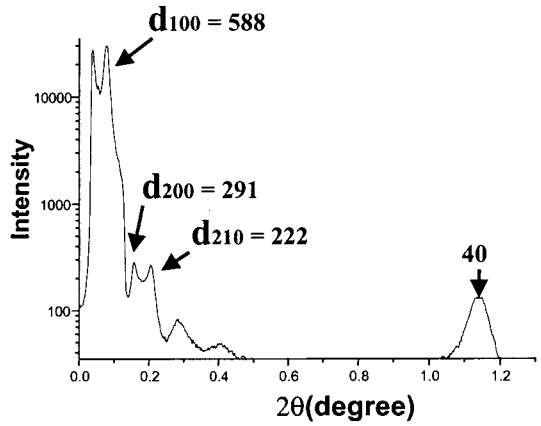

Figure 5. One-dimensional, room temperature line scan of BC-2A0.66F8H10 of the SAXS pattern shown in Figure 4.

characteristic of hexagonally packed structures. The domain spacing calculated from SAXS of 680 Å is in good agreement with TEM data.

Unlike coil−coil block copolymers, the side chain 2-armed monodendron LC−coil block copolymer can self-assemble on several length scales. Within the LC microdomains, which are discussed in the next section, the side-chain LC mesogens form a confined smectic B mesophase as shown by DSC and WAXS. To understand how the mesophase is aligned with respect to the microdomain structure, additional two-dimensional X-ray patterns (Figure 6) of the same macroscopically oriented film were taken. This pattern shows a set of inner Bragg reflections resulting from the hexagonally packed cylinders and a pair of outer reflections resulting from the smectic B mesophase. Obviously, the smectic layer reflections are perpendicular to the PS−cylinder reflections. From Figure 2, we know that mesogen alignment is perpendicular to the smectic layers. As a result, the X-ray studies demonstrate that these side chain LC mesogens have a homogeneous boundary condition in the bulk with respect to the intermaterial dividing surface and are oriented in the axis direction

Table 3. Water Contact Angles and Critical Surface Tensions of Selected Semifluorinated Block Copolymers Polymers with Monodendron Side Groups

polymer[a]	monodendron	attachment ratio (%)	advancing angle (deg)	receding angle (deg)	critical surface tension (mN/m)
BC-2A0.62F8H6	A_2-F_8H_6	68.2	121	103	9.2
BC-2A0.66F8H10	A_2-F_8H_{10}	66.3	121	108	8.1
BC-2A0.38F10H10	A_2-$F_{10}H_{10}$	38.0	122	110	8.2
BC-3A0.24F8H10	A_3-F_8H_{10}	23.7	117	98	9.1
BC-3A0.53F8H10	A_3-F_8H_{10}	53.1	120	108	8.5
BC3A0.58F10H10	A_3-$F_{10}H_{10}$	57.5	124	110	7.7

[a] BC denotes block copolymer, FxHy refers to the composition of the semifluorinated group, and 0.*zz* indicates the extent of attachment on the hydroxylated backbone.

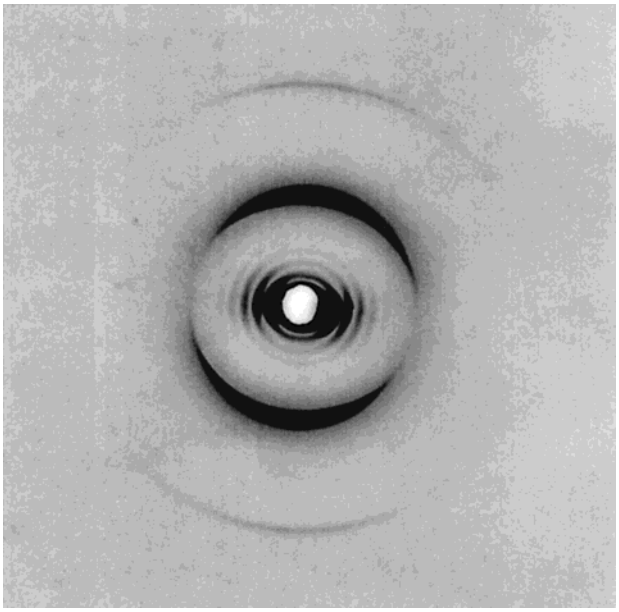

Figure 6. WAXD pattern of BC-2A0.66F8H10. The reflections due to the smectic layers are oriented normal to the reflections of the cylinders (monochromatic wavelength = 1.54 Å; sample-to-detector distance = 144 mm).

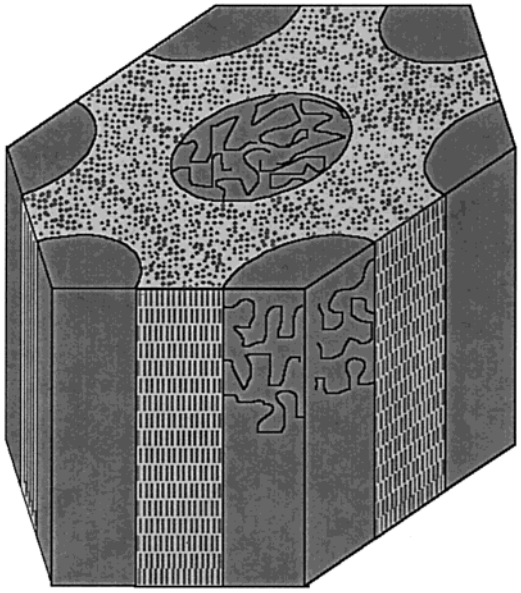

Figure 7. Schematic model for the coupled microstructure and LC organization of BC-2A0.66F8H10. Cylinders are polystyrene phase.

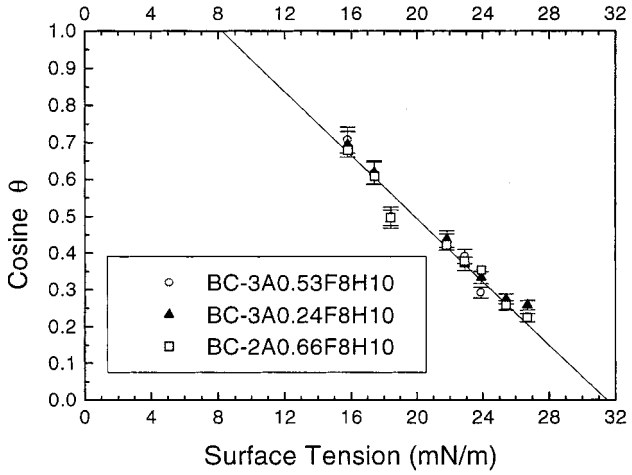

Figure 8. Zisman plot of semifluorinated block copolymers with selected 2- and 3-armed monodendron side groups [polymers BC-3A0.53F8H10 (53%), BC-3A0.24F8H10 (24%), and BC-2A0.66F8H10 (66%) with different extents of attachment and monodendron structure but the same F_8H_{10} SF group].

of the cylinders. Combining the WAXS, SAXS, and TEM results for this block copolymer, we propose a schematic molecular model shown in Figure 7, which illustrates the packing between the side group LC monodendrons and the coil chains. This packing behavior is consistent with observations made by others and us for polymers with single LC side groups[5] but is remarkable in view of the fact this complex structure is observed with side group monodendrons. It should be noted that not all side group LC block copolymers show this orientation in thin film studies.

Critical Surface Tension. The critical surface tension of these polymers and their stability were evaluated and are reported in Table 3. It is well-known that the contact angle of a liquid on a given low-energy surface usually increases with surface tension except when the liquid has a tendency to dissolve or reorganize the surface molecules of the wetted solid. Using as standards a series of linear alkanes and two low molecular weight trimethylsilyl-terminated poly(dimethylsiloxane)s with known surface tension, the advancing contact angles were measured. Values of critical surface tension were extrapolated from Zisman plots of cos(θ) versus surface tension as shown in Figure 8.

Provided that $-CF_2-$ lengths longer than eight were used, it was found that all block copolymers with monodendron side groups have surface energies in the range 7−9 mJ/m^2 regardless of either the extent of attachment (which varied from 25% to 70%) or the monodendron structure. These values are comparable to values obtained for similar block copolymers with single semifluorinated side groups[5] and are very close to the known critical surface tension of a uniform $-CF_3$ surface formed by monolayers of perfluorocarbon acids (e.g., 8.6 mJ/m^2 for perfluorohexanoic acid and 7.9 mJ/m^2 for perfluorooctanoic acid).[33] Since those monolayers

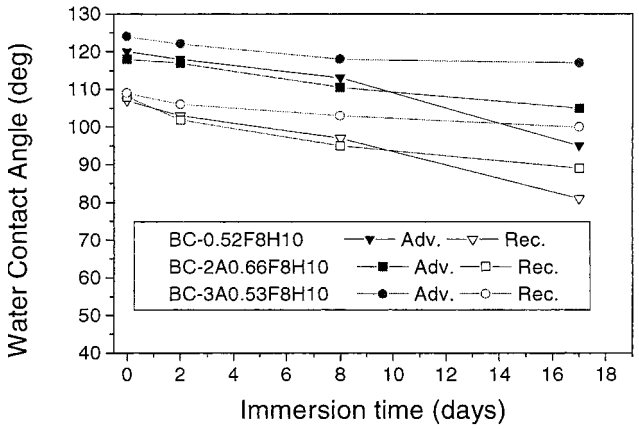

Figure 9. Time dependence of the advancing and receding water contact angles of semifluorinated block copolymers [BC-0.52F8H10 (52%), BC-3A0.24F8H10 (24%), and BC-3A0.53F8H10 (53%) F_8H_{10} SF group].

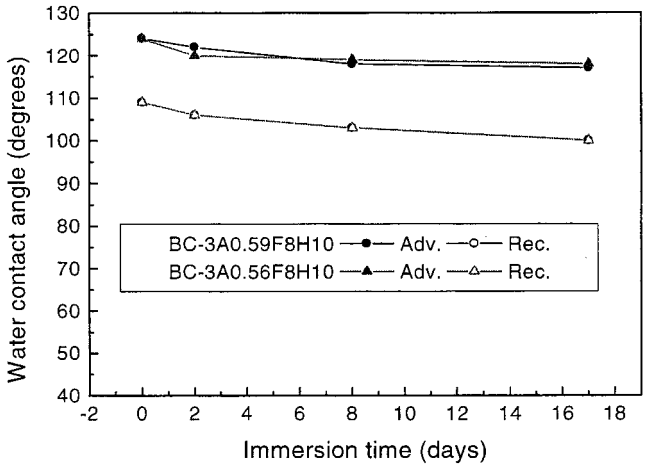

Figure 10. Comparison of surface stability of semifluorinated block copolymer with the same mesogen length and different non-SF segment lengths [BC-3A0.59F8H10 (38K PS−5.5K SF), BC-3A0.56F8H10 (66K PS−6.7K SF)].

have vertically oriented and closely packed perfluorinated chains, we may infer that these polymer surfaces have similar orientation and packing of their perfluorinated segments and that hydrophobic $-CF_3$ groups are well organized on the surface, while the more hydrophilic OH and ester groups are almost completely hidden by the low surface energy monodendron structure.

Effect of Side Groups on the Temporal Stability of the Surface. For a hydrophobic coating material used under a polar environment, it is very important to understand the long-term surface stability of these polymer films. For this purpose, partially substituted block copolymers with single semifluorinated side groups were synthesized for comparison with polymers having 2-armed and 3-armed monodendrons. The attachment ratios for all side group types were controlled to be ~55% so that the residual OH molar ratio in all polymers remained the same. Obviously, the fluorinated unit content in each polymer is quite different; i.e., 3-armed polymers have the highest content, while the single chain polymers have the lowest. The contact angle changes versus immersion time of polymer films in water over a 2 week period are shown in Figure 9.

The advancing contact angle for single semifluorinated side groups drops slightly over this period, while only 12° and 5° respectively for the 2-armed polymer and 3-armed polymers. A similar situation is found for the receding contact angle. From DSC measurements, the semifluorinated chains in the partially substituted single SF group polymers (BC-0.52F8H10) are unable to form a well-ordered smectic mesophase as demonstrated by both transition temperature and enthalpy. Therefore, it is difficult for the single side groups to prevent penetration of water into the film and avoid surface reconstruction. Despite this, the surface is still dominated by C−F and C−H bonds, and not OH groups, because the contact angles are still relatively high. A major improvement in hydrophobic properties can be found by using the 2-armed monodendron. Any change in advancing and receding contact angles decreases substantially, because the much larger fluorinated groups more efficiently cover the polymer surface and formation of the stable smectic B mesophase is more readily achieved. With 3-armed monodendron side groups, a very stable and hydrophobic surface is formed. During the 2 week period of immersion, there was a reduction of only a few degrees for both advancing and receding contact angles even though 45% of attachment sites were still OH groups. Thus, the higher the transition temperature and enthalpy associated with loss of the mesophase, the more stable the surface remains. Undoubtedly, block copolymers with this kind of monodendron structure are effective at creating a stable, low-energy surface and effective at masking underlying polar groups, such as OH groups. This experiment also indicates that such monodendron units may be effectively used for surface modification without the need for regularly arranged attachment sites.

As demonstrated above, a 3-armed monodendron structure with $-CF_2-$ length of 8 or more carbons was found to have the best masking effect on the underlying polar groups. The longest $-CF_2-$ mesogen (10 carbons long) was used in this comparison in order to enhance surface stability. As shown in Figure 10, higher advancing contact angle and greater stability during immersion in water were observed for block copolymers with the longer mesogen lengths, thus indicating a more stable surface. Another important factor on surface stability is the attachment ratio or degree of attachment. Figure 10 also shows that the extent of attachment can dramatically affect surface stability. By reducing the attachment of 3-armed monodendron from 58.5% (BC-3A0.59F8H10) to 23.7% (BC-3A0.24F8H10) of available hydroxy groups, surface stability can be compromised. Observed contact angles of BC-3A0.24F8H10 decreased about 20°−30° during immersion which demonstrates the instability of its surface. A reduced degree of LC organization as shown by lower transition enthalpies and temperatures of the LC state also resulted from the low degree of attachment and is presumably responsible for the inability of the surface to resist reconstruction.

NEXAFS Measurements of the Orientational Order of the Semifluorinated Groups. The surface structure of these semifluorinated polymers was further characterized by near edge X-ray absorption fine structure (NEXAFS) analysis. Details of this work appear elsewhere.[12,34,35] The orientation of the semifluorinated units in the near surface region (upper 2 nm) was by examining the partial electron yield signals. From these we conclude that the surface is entirely dominated by the fluorocarbon segments and that their net orientation in the surface region is toward the surface normal, thus forming a $-CF_3$ surface. This fact can be established

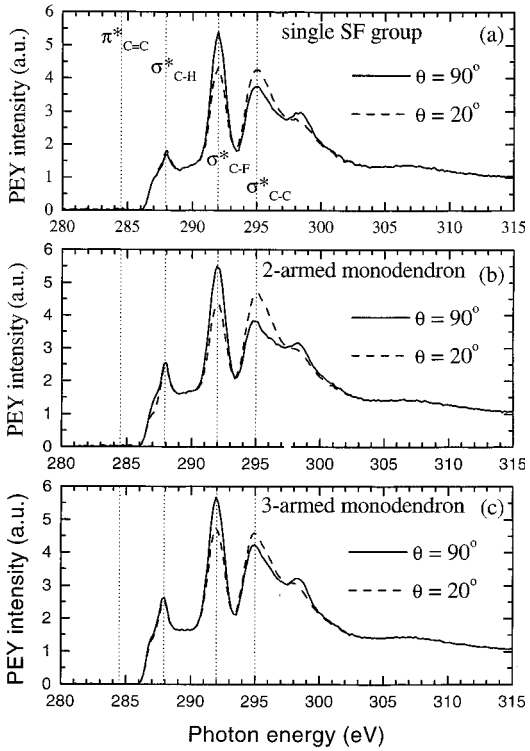

Figure 11. NEXAFS partial electron yield intensity versus X-ray photon energy for angles θ between the electric field vector of the polarized X-rays and the sample normal of 90° and 20°: (a) sample BC-0.99F8H10 (single SF groups), (b) sample BC-2A0.66F8H10 (2-armed monodendrons), and (c) sample BC-3A0.59F8H10 (3-armed monodendrons).

qualitatively by comparing the partial electron yield results at two different incident angles of 20° and 90° in the NEXAFS data. Figure 11a shows the partial electron yield (PEY) signal as a function of soft X-ray photon energy over the region of the C K-edge for the single SF group substituted block copolymer while parts b and c of Figure 11 show similar data for the 2-armed and 3-armed monodendrons (BC-2A0.66F8H10 and BC-3A0.59F8H10), respectively. Two curves are shown on each plot, one corresponding to an angle θ between the electric field vector **E** of the polarized X-ray beam and the surface normal of 90° and one corresponding to an angle θ of 20°. Although the 1s to π^* (E = 284.5 eV) resonant transition is the strongest feature of the X-ray fluorescence yield spectrum of each of these samples, there is only a small 1s to π^* PEY signal from the phenyl rings of the polystyrene (PS) block in any of these plots. The absence of this resonance in the PEY spectrum means that there is almost no PS within 2 nm of the surface of any of these samples; i.e., the sample surfaces consist almost exclusively of the semifluorinated isoprene block.

Also marked on each plot are the resonant energies of the 1s → σ^* transitions for the C−H (E = 287.9 eV), C−F (E = 292.0 eV), and C−C (E = 295.0 eV) bonds. In all cases the $C-F_{1s\rightarrow\sigma^*}$ PEY signal is larger at θ = 90° than at θ = 20° while the $C-C_{1s\rightarrow\sigma^*}$ PEY signal is larger at θ = 20° than at θ = 90°. The PEY spectra, which were measured at the intermediate angles of θ = 30°, 40°, 55°, 60°, 70°, and 80°, lie between the 90° and 20° extremes but are not shown in Figure 11a−c for clarity. The spectra show that in all samples there is some orientational order of the C−F and C−C bonds near the surface. The fact that the $C-F_{1s\rightarrow\sigma^*}$ PEY signal is larger at θ = 90° than at θ = 20° means that the C−F bonds

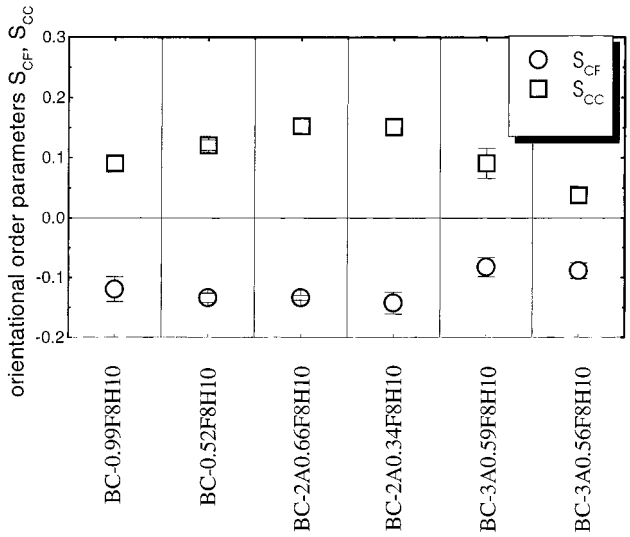

Figure 12. Orientational order parameters for C−F σ-bonds and C−C σ-bonds at surfaces made up of single SF groups (BC-0.99F8H10 and BC-0.52F8H10), 2-armed monodendrons (BC-2A0.66F8H10 and BC-2A0.34F8H10), and 3-armed mondendrons (BC-3A0.59F8H10 and BC-3A0.56F8H10).

are at least somewhat oriented parallel to the plane of the sample surface whereas the anisotropy in the $C-C_{1s\rightarrow\sigma^*}$ PEY signal means that these bonds have some net orientation normal to the sample surface. These results are consistent with previous ones on the semifluorinated LC block copolymers[12,33,34] and indicate that the rigid $-CF_2-$ helix is, on the average, oriented normal to the sample surface. The degree of that orientation or the orientational order, however, is clearly different for the different samples. The surface of the 3-armed monodendrons is clearly less oriented than that of the 2-armed monodendrons while the surface of the 2-armed monodendrons is about as oriented as those of the single SF group substituted block copolymer.

To quantify these statements, we have analyzed these NEXAFS data as described in the Appendix to determine the uniaxial order parameters S_{CF} and S_{CC} of the CF and CC bonds of the surface. These range from +1 (σ bond axis completely aligned along z) to $-1/2$ (σ bond axis lying in the plane of the surface) and are equivalent to the Hermans orientation function of X-ray diffraction.[36] These are shown in Figure 12. In addition, we have computed from these the uniaxial orientational order parameter S_{helix} of the $-CF_2-$ helix as well as the average angle between the helix and the surface normal. These are given in Table 4 along with the other order parameters. It can be seen that the CF and CC order parameters for all samples are comparable in magnitude but different in sign, with S_{CF} being negative and S_{CC} being positive. The C−F helix order parameter computed from S_{CF} is approximately 0.26 for both the two single SF side group block copolymers and the two 2-armed monodendron block copolymers even though the two polymers with single SF side groups and the two polymers with 2-armed monodendrons have quite different attachment ratios (0.99 for BC-0.99F8H10 vs 0.52 for the BC-0.52F8H10 and 0.66 for the BC-2A0.66F8H10 vs 0.34 for the BC-2A0.34F8H10). Therefore, even large differences in attachment ratio do not seem to produce large differences in orientational order of the semifluorinated mesogen surfaces. The surface orientational order parameter of the $-CF_2-$ helix for the two block copolymer with attached 3-armed mono-

Table 4. Surface Orientational Order Parameters and Average Helix Angles Determined from NEXAFS

polymer	S (C−F σ-bond)	S (C−C σ-bond)	S_{helix} (−CF_2− helix)	$\langle\tau_{F-helix}\rangle$ (deg)
BC-0.99F8H10	−0.120 ± 0.021	0.090 ± 0.011	0.240 ± 0.042	45.4 ± 1.6
BC-0.52F8H10	−0.134 ± 0.008	0.121 ± 0.009	0.268 ± 0.016	44.3 ± 0.6
BC-2A0.66F8H10	−0.134 ± 0.004	0.153 ± 0.012	0.268 ± 0.008	44.3 ± 0.3
BC-2A0.34F8H10	−0.143 ± 0.018	0.151 ± 0.015	0.286 ± 0.036	43.7 ± 1.4
BC-3A0.59F8H10	−0.082 ± 0.016	0.091 ± 0.025	0.164 ± 0.032	48.3 ± 1.2
BC-3A0.56F8H10	−0.088 ± 0.013	0.038 ± 0.011	0.176 ± 0.026	47.8 ± 1.0

dendrons, however, is significantly smaller, about 0.17.

The smaller CF helix order parameter for the 3-armed monodendron surfaces may be related to the fact that these surfaces show roughness on a scale of about 10 nm (observed by SFM) that is significantly larger than that for the 2-armed monodendron and single SF side group surfaces. The 3-armed SF monodendron polymers have a surface consisting of spherical humps about 10 nm in diameter. This topography may be due to spontaneous curvature of the surface region caused by the frustration introduced by attaching these bulky monodendrons to the polymer backbone. The observed effect of these surface textures on wetting is negligible, since all these polymer surfaces show similar advancing and receding water contact angles on fresh exposure to water. The spontaneous curvature may however affect the NEXAFS results, since the extra surface roughness should introduce an extra source of orientational disorder. In addition, the packing frustration that we speculate gives rise to the fine scale surface topology may introduce an extra splay in the surface smectic director that that will result in poorer orientational order.

Conclusions

In summary, a series of styrene-modified diene block copolymers with low surface energy, semifluorinated monodendron side groups were prepared and studied by a variety of methods. A general procedure for synthesizing low-energy surface forming semifluorinated monodendrons has been developed which can be extended to the synthesis of higher generation monodendrons. The surface of the block copolymer films examined in this study is largely made up of a uniform $-CF_3$ layer and typically has surface energies of only 7−9 mJ/m^2. The molecular structure of the monodendrons plays an important role in surface stability. In particular, the linking of the monodendron core and the fluorinated mesogen by a flexible group determines the temperature and enthalpy of a smectic B−isotropic transition present in these polymers, which in turn controls resistance to surface reconstruction. With sufficiently long methylene spacers and mesogenic groups, the polymer film surface is stabilized by the LC mesophase and can resist reconstruction in water even with hydrophilic OH groups lying just beneath the surface. Studies of the effect of degree of substitution on surface stability showed that the more arms on the monodendron, the more it could tolerate partial substitution and still form a stable low-energy surface. Thus, the use of the semifluorinated monodendron structure is a promising strategy for creation of stable, low-surface-energy materials with strong subsurface polar group masking ability.

Acknowledgment. The primary support of the Office of Naval Research (Grant N00014-95-1-0695) and partial support by National Science Foundation, Division of Materials Research, Polymers Program under Grants DMR98-03738, DMR93-21573, and DMR93-214573 are gratefully acknowledged. The work at NCSU was supported by start-up funds from NCSU and from a NSF Career Award to J.G. We also acknowledge Cornell High Energy Synchrotron Source (CHESS) and the Cornell Center for Materials Research (CCMR). NEXAFS experiments were carried out at the National Synchrotron Light Source, Brookhaven National Laboratory, which is supported by the U.S. Department of Energy, Division of Materials Sciences and Division of Chemical Sciences. Valuable discussions with Dr. Jianguo Wang (Corning Inc.), Dr. Guoping Mao (3M Austin Center), and Dr. Birgit Glüsen (Hüls) are gratefully acknowledged as well as the experimental assistance of Dr. Robert A. Bubeck, Dr. Sharadha Sambasivan, and Yushi Ando.

Appendix: The Orientational Order Parameter

The orientational order is found by first using the method of Outka and co-workers[37] to fit the PEY NEXAFS spectra as a series of Gaussian curves representing the different 1s → σ^* transitions and a step function corresponding to the excitation edge of carbon. The magnitudes of these Gaussians are taken to be the intensities $I(\theta)$ of the various 1s → σ^* transitions. Using the notation of Stöhr and Samant,[38] the molecular orientation factors f_x, f_y, and f_z for the C−F and C−C bonds are defined as follows:

$$f_z = \int \cos^2 \alpha \, f(\alpha) \, d\Omega$$

$$f_x = f_y = \frac{1 - f_z}{2}$$

where z is an axis normal to the film surface and x and y are orthogonal axes in the plane of the surface while α is the angle between the axis of the σ^* orbital (σ bond axis) and z. The molecular axis distribution function $f(\alpha)$ is normalized so that $\int f(\alpha) \, d\Omega = 1$ and thus $f_x + f_y + f_z = 1$. A uniaxial orientation order parameter S is then defined as

$$S = \frac{1}{2}(3f_z - 1) \qquad (1)$$

where S ranges from +1 (σ bond axis completely aligned along z) to $-1/2$ (σ bond axis lying in the plane of the surface). It is assumed that there is isotropy in the plane of the surface; i.e., there is no preferred direction in the plane. The order parameter defined in this way is analogous to the Hermans orientation parameter of X-ray diffraction.[36]

Regardless of the amount of orientation of the σ bond normal to the plane, the PEY intensity $I(\theta)$ is predicted to have the following form:

$$I(\theta) = A + B \sin^2 \theta \qquad (2)$$

The orientational order parameter S can be determined

from the values of A and B[19] as follows:

$$S = -\frac{P^{-1}B}{3A + (3 - P^{-1})B} \tag{3}$$

where P is the polarization factor of the X-ray beam (0.85 in our case).

Previously we reported the average tilt angle $\langle\tau_{F-helix}\rangle$ of the fluorocarbon helix part of single semifluorinated groups with respect to the surface normal[34] which was calculated on the basis of the "building block model".[37,39] This average tilt angle is directly related to the orientational order parameter of the C−F bonds, S_{CF}, as follows:

$$S_{CF} = \frac{1}{2}\left(\frac{3}{2}\sin^2\langle\tau_{F-helix}\rangle - 1\right) \tag{4}$$

Inversion of eq 4 yields $\langle\tau_{F-helix}\rangle$ values from values of S_{CF}, and these values of $\langle\tau_{F-helix}\rangle$ are also given in Table 4. Finally, the order parameter S_{helix} of the $-CF_2-$ helix axis relative the surface normal is given by

$$S_{helix} \equiv -2S_{CF}$$

References and Notes

(1) Bernett, M. K.; Zisman, W. A. *J. Phys. Chem.* **1962**, *62*, 1207.
(2) (a) Doeff, M. M.; Lindner, E. *Macromolecules* **1989**, *22*, 2951. (b) Lindner, E. *Biofouling* **1992**, *6*, 193.
(3) Thomas, R. R.; Anton, D. R.; Graham, W. F.; Darman, M. J.; Sauer, B. B.; Stika, K. M.; Swartzfager, D. G. *Macromolecules* **1997**, *30*, 2883.
(4) Mera, A. E.; Wynne, K. J. *Polym. Prepr. (ACS Polym. Chem. Div.)* **1998**, *39* (2), 806.
(5) Wang, J.-G.; Mao, G.-P.; Ober, C. K.; Kramer, E. J. *Macromolecules* **1997**, *30*, 1906.
(6) Beyou, E.; Babin, P.; Bennetau, B.; Dunogues, J.; Teyssie, D.; Boileau, S. *J. Polym. Sci., Polym. Chem.* **1994**, *32*, 1673. (b) Beyou, E.; Bennetau, B.; Dunogues, J.; Babin, P.; Teyssie, D.; Boileau, S.; Corpart, J. M. *Polym. Int.* **1995**, *38*, 237.
(7) Rabolt, J. F.; Russell, R. T.; Twieg, R. J. *Macromolecules* **1984**, *17*, 2786.
(8) Mahler, W.; Fuillon, D.; Skoulios, A. *Mol. Cryst. Liq. Cryst. Lett.* **1985**, *2*, 111.
(9) Viney, C.; Twieg, R. J.; Russell, R. T.; Depero, L. E. *Liq. Cryst.* **1989**, *5*, 1783.
(10) Krupers, M.; Moller, M. *Macromol. Chem. Phys.* **1997**, *198*, 2163.
(11) Percec, V.; Lee, M. *J. Macromol. Sci., Pure Appl. Chem.* **1992**, *A29* (9), 723.
(12) Genzer, J.; Sivaniah, E.; Kramer, E. J.; Wang, J.; Xiang, M.; Char, K.; Ober, C. K.; Bubeck, R. A.; Fischer, D. A.; Graupe, M.; Colorado, R.; Shmakova, O. E.; Lee, T. R. *Macromolecules*, in press.
(13) Perutz, S. M.; Wang, J.; Kramer, E. J.; Ober, C. K.; Ellis, K. *Macromolecules* **1998**, *31*, 4272.
(14) Wang, J.; Ober, C. K. *Macromolecules* **1997**, *30*, 7560.
(15) Tully, D. C.; Wilder, K.; Fréchet, J. M. J.; Trimble, A. R.; Quate, C. F. *Adv. Mater.* **1999**, *11*, 314.
(16) Ihre, H.; Hult, A.; Soderlind, E. *J. Am. Chem. Soc.* **1996**, *118*, 6388.
(17) Newkome, G. R.; Arai, S.; Fronczek, F. R.; Moorefield, C. N.; Lin, X. F.; Weis, C. D. *J. Org. Chem.* **1993**, *58*, 898.
(18) Mao, G.-P.; Wang, J.-G.; Clingman, S. R.; Ober, C. K.; Chen, J. T.; Thomas, E. L. *Macromolecules* **1997**, *30*, 2556.
(19) Zisman, W. A. *Contact Angle, Wettability, and Adhesion*; American Chemical Society: Washington, DC, 1964.
(20) Davis, R.; Muchowski, J. M. *Synthesis* **1982**, 987.
(21) Pfeffer, P. E.; Silbert, L. S. *J. Org. Chem.* **1976**, *41*, 1373.
(22) Price, C. In *Developments in Block Copolymers*; Goodman, I., Ed.; Elsevier Applied Science Publisher: London, 1982; Chapter 2.
(23) Hawker, C. J. *Adv. Polym. Sci.* **1999**, *147*, 113.
(24) Hawker, C. J.; Farrington, P. J.; Mackay, M. E.; Wooley, K. L.; Frechet, J. M. J. *J. Am. Chem. Soc.* **1995**, *117*, 4409.
(25) Percec, V.; Ahn, C.-H.; Cho, W.-D.; Jamieson, A. M.; Kim, J.; Leman, T.; Schmidt, M.; Gerle, M.; Moeller, M.; Prokhorova, S. A.; Sheiko, S. S.; Cheng, S. Z. D.; Zhang, A.; Ungar, G.; Yeardley, D. J. P. *J. Am. Chem. Soc.* **1998**, *120*, 8619.
(26) Iyer, J.; Hammond, P. T. *Langmuir* **1999**, *15*, 1299.
(27) Iyer, J.; Fleming, K.; Hammond, P. T. *Macromolecules* **1998**, *31*, 8757.
(28) Cooper, A. I.; Londono, J. D.; Wignall, G.; McClain, J. B.; Samulski, E. T.; Lin, J. S.; Dobrynin, A.; Rubinstein, M.; Burke, A. L.; Fréchet, J. M. J.; Desimone, J. M. *Nature* **1997**, *389*, 368.
(29) Johansson, G.; Percec, V.; Ungar, G.; Zhou, J. P. *Macromolecules* **1996**, *29*, 646.
(30) Percec, V.; Johansson, G.; Ungar, G.; Zhou, J. *J. Am. Chem. Soc.* **1996**, *118*, 9855.
(31) Percec, V.; Cho, W. D.; Mosier, P. E.; Ungar, G.; Yeardley, D. J. P. *J. Am. Chem. Soc.* **1998**, *120*, 11061.
(32) (a) Stebani, U.; Lattermann, G. *Adv. Mater.* **1995**, *7*, 578. (b) Cameron, J. H.; Facher, A.; Lattermann, G.; Diele, S. *Adv. Mater.* **1997**, *9*, 398.
(33) Hare, E. F.; Shafrin, E. G.; Zisman, W. A. *J. Phys. Chem.* **1954**, *58*, 236.
(34) Genzer, J.; Sivaniah, E.; Kramer, E. J.; Wang, J.; Körner, H.; Xiang, M.; Char, K.; Ober, C. K.; DeKoven, B. M.; Bubeck, R. A.; Chaudhury, M. K.; Sambasivan, S.; Fischer, D. A. *Macromolecules* **2000**, *33*, 1882.
(35) Genzer, J.; Sivaniah, E.; Kramer, E. J.; Wang, J.; Körner, H.; Char, K.; Ober, C. K.; DeKoven, B. M.; Bubeck, R. A.; Fischer, D. A.; Sambasivan, S. *Langmuir* **2000**, *16*, 1993.
(36) Donald, A. M.; Windle, A. H. *Liquid Crystalline Polymers*; Cambridge University Press: Cambridge, 1992. Alexander, L. E. *X-Ray Diffraction Methods in Polymer Science*; R. E. Krieger Publishing: Huntington, NY, 1979.
(37) Outka, D.; Stöhr, J.; Rabe, J.; Swalen, J. D. *J. Chem. Phys.* **1988**, *88*, 4076.
(38) Stöhr, J.; Samant, M. G. *J. Electron Spectrosc. Relat. Phenom.* **1999**, *98*−*99*, 189.
(39) Stöhr, J. *NEXAFS Spectroscopy*; Springer-Verlag: Berlin, 1992.

MA992111S